Letter

Decoupling multiphase superconductivity from normal state ordering in $CeRh_2As_2$

K. Semeniuk,[1,*] D. Hafner,[1] P. Khanenko,[1] T. Lühmann,[1] J. Banda,[1] J. F. Landaeta,[1] C. Geibel,[1] S. Khim,[1] E. Hassinger,[2,†] and M. Brando[1,‡]

[1]*Max Planck Institute for Chemical Physics of Solids, D-01187 Dresden, Germany*

[2]*TUD Dresden University of Technology, Institute for Solid State and Materials Physics, D-01062 Dresden, Germany*

(Received 20 January 2023; revised 21 April 2023; accepted 7 June 2023; published 20 June 2023)

$CeRh_2As_2$ is a multiphase superconductor with $T_c = 0.26$ K. The two superconducting (SC) phases, SC1 and SC2, observed for a magnetic field H parallel to the c axis of the tetragonal unit cell, have been interpreted as even- and odd-parity SC states, separated by a phase boundary at $\mu_0 H^* = 4$ T. Such parity switching is possible due to a strong Rashba spin-orbit coupling at the Ce sites located in locally noncentrosymmetric environments of the globally centrosymmetric lattice. The existence of another ordered state (phase I) below a temperature $T_0 \approx 0.4$ K suggests an alternative interpretation of the H^* transition: It separates a mixed SC+I (SC1) and a pure SC (SC2) state. Here, we present a detailed study of higher-quality single crystals of $CeRh_2As_2$, showing much sharper signatures at $T_c = 0.31$ K and $T_0 = 0.48$ K. We refine the T-H phase diagram of $CeRh_2As_2$ and demonstrate that $T_0(H)$ and $T_c(H)$ lines meet at $\mu_0 H \approx 6$ T, well above H^*, implying no influence of phase I on the SC phase switching. A basic analysis with the Ginzburg-Landau theory indicates a weak competition between the two orders.

DOI: 10.1103/PhysRevB.107.L220504

$CeRh_2As_2$ is a newly discovered heavy-fermion superconductor with remarkable properties. At temperatures below $T_c = 0.26$ K, the material shows an exceptionally rare multiphase superconductivity [1]. Apart from UPt_3 [2–4] and UTe_2 [5–8], virtually all other unconventional superconductors host only one superconducting (SC) state. Above T_c, the compound shows a non-Fermi-liquid temperature dependence of specific heat, $C/T \propto T^{-0.6}$, and electrical resistivity, $\rho(T) \propto \sqrt{T}$, suggesting proximity to a quantum critical point (QCP) of unknown nature [1] or influence of two-channel Kondo physics [9]. Below the temperature of $T_0 \approx 0.4$ K, the material also hosts a peculiar state, phase I, proposed to be a unique case of a quadrupole-density-wave (QDW) order [10], contrasting all known multipolar orders observed in Ce-based systems which are typically of local origin [11,12]. Moreover, very recent nuclear quadrupolar and magnetic resonance experiments report broadening of the As lines below $T_N < T_c$ at one of the two As sites, indicating the presence of internal fields, likely due to an antiferromagnetic (AFM) order in one of the two SC phases [13,14].

In fact, $CeRh_2As_2$ shows a single SC phase when magnetic field is applied along the basal plane of the tetragonal crystalline structure, but two SC phases, SC1 and SC2, for a field H parallel to the c axis (the relevant field direction for the rest of this Letter). These phases are separated by a boundary at $\mu_0 H^* = 4$ T, as shown in Fig. 1. The anisotropic field response of the superconductivity, as well as the presence of two SC phases in $CeRh_2As_2$ can be attributed to a strong Rashba spin-orbit coupling due to the locally noncentrosymmetric environments of Ce sites and quasi-two-dimensional character of the Fermi surface (FS) [1,10,16]. The existing model is based on a scenario proposed ten years ago for layered structures comprising loosely coupled superconducting layers with alternating sign of the Rashba spin-orbit coupling. Such systems were predicted to exhibit a SC phase diagram very similar to that observed in $CeRh_2As_2$ [16–23], with the SC1-SC2 transition being a first-order phase transition between even- and odd-parity SC order parameters [1]. In the case of $CeRh_2As_2$, such an interpretation is also corroborated by the angle dependence of the SC upper critical field [15].

Besides the parity switching, there currently exist two alternative explanations for the multiphase superconductivity in $CeRh_2As_2$: (1) a field-induced magnetic transition within the SC state [24], in line with a recent NMR study [14], and loosely reminiscent of the case of high-pressure $CeSb_2$ [25], and (2) a transition between a mixed SC+I state (SC1) and a pure SC state (SC2). As illustrated in Fig. 1, the $T_0(H)$ line curves towards lower temperature with increasing field and seems to vanish near the $T_c(H^*)$ critical point [1,15,26]. If the second scenario is valid, all four phase boundaries should meet at a single multicritical point. This can be verified by refining the phase diagram of $CeRh_2As_2$. The topology of the phase diagram close to the $T_c(H^*)$ point also has important thermodynamic implications. If the $T_0(H)$ and $T_c(H)$ lines meet at $H > H^*$, the SC1-SC2 boundary must be of first order

*Corresponding author: konstantin.semeniuk@cpfs.mpg.de
†Corresponding author: elena.hassinger@tu-dresden.de
‡Corresponding author: manuel.brando@cpfs.mpg.de

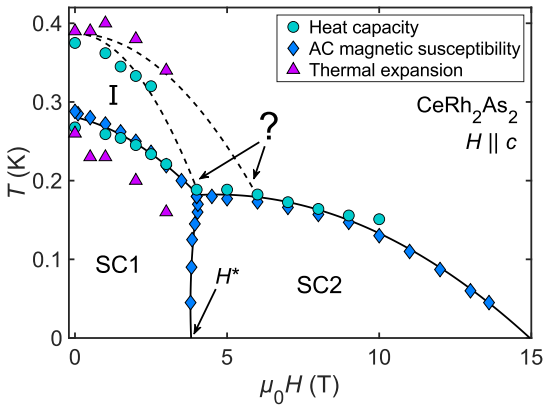

FIG. 1. Temperature–c-axis magnetic field (T-H) phase diagram of $CeRh_2As_2$ according to magnetic and thermodynamic bulk probes. All measurements were conducted before this work, on the same batch of crystals (published in Refs. [1,15], except the thermal expansion). The dashed lines highlight the ambiguity of the phase diagram: The phase-I transition line may meet the superconducting region either at the multicritical point at $\mu_0 H^* = 4$ T, or at some higher field.

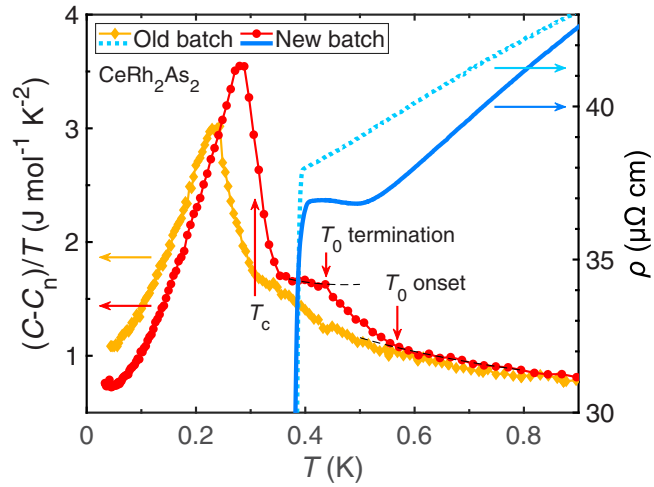

FIG. 2. Specific heat $C(T)/T$ and resistivity $\rho(T)$ of $CeRh_2As_2$ as functions of temperature T showing signatures of the superconductivity and phase I (T_c and T_0, respectively) for two different generations of samples ("old batch" denotes the samples used in Refs. [1,10,15], while samples from the "new batch" were used in this work). The dashed black lines extrapolate sections of $C(T)/T$ for emphasizing the phase-I transition. The nuclear specific heat contribution $C_n(T)$ due to As atoms was subtracted (see the Supplemental Material [28]). Resistivity of the old batch sample is scaled by a factor of 0.6.

[27], and the two SC states must have distinct symmetries. These reasonings would hold regardless of the microscopic nature of phase I.

In our experiments so far, insufficient sample homogeneity and broadening of features in magnetic field prevented us from reliably tracking the phase-I boundary close to the multicritical point. Progress on this front therefore demands samples of higher quality.

Here, we report a detailed study of specific heat and electrical resistivity of higher-quality single crystals of $CeRh_2As_2$ with $T_c = 0.31$ K and $T_0 = 0.48$ K, which exhibit much clearer signatures of the phase transitions. We refine the T-H phase diagram of $CeRh_2As_2$ and demonstrate that the phase-I boundary meets the SC state at around 6 T—a significantly larger field than H^*—thus decoupling the SC1-SC2 switching and the presence of phase I. We do not observe any signatures of T_0 above 6 T within the SC2 phase, yet the sudden disappearance of the phase I at the SC2 phase boundary would go against thermodynamic principles. We also do not detect any signatures of magnetic transition within the SC states.

A significant improvement of the sample quality is illustrated in Fig. 2, where thermodynamic and transport signatures of T_0 and T_c are compared for the samples of $CeRh_2As_2$ used in Refs. [1,10,15,29] (old batch) and the new generation of samples studied in this Letter [referred to as the new batch, whose synthesis is outlined in the Supplemental Material (SM) [28]]. One can identify two specific heat [$C(T)$] anomalies—the larger jump due to the SC transition and the smaller phase-I anomaly—both of which appear as typical second-order phase transitions, affected by broadening. Samples of the new batch show a higher bulk T_c (0.31 K against 0.26 K) with a much sharper peak in specific heat, indicating a substantially improved homogeneity of crystals. The height of the jump at T_c is $\Delta C/C|_{T_c} \approx 1.3$, whereas the value of 1 was reported for the old samples [1]. The Sommerfeld coefficient $\gamma = C/T$ for $T \to 0$ decreases to 0.7 J K^{-2} mol^{-1} in the new sample, which is a 40% reduction compared to the previous value of about 1.2 J K^{-2} mol^{-1} [1], signifying a particularly strong sensitivity of superconductivity to disorder. The phase-I transition is likewise more pronounced, with its onset and termination clearly visible as changes in the slope of $C(T)/T$. The strong increase of T_0 from 0.4 to 0.48 K with increasing sample quality is consistent with an itinerant nature of a sign changing order in k space such as the proposed QDW.

Measurements of electrical resistivity [$\rho(T)$] reveal a visibly higher T_c compared to the bulk value, reflecting the inhomogeneity of samples, also seen in other heavy-fermion systems [30]. The discrepancy is reduced for the new batch, as the resistive T_c of 0.38 K is effectively the same as for the old batch [1,10]. More importantly, the higher T_0 in the new batch makes the corresponding transport signature (resistivity upturn) much more apparent. Measurements of $\rho(T)$ can therefore be used for tracing the boundary of phase I, which was rather challenging previously, as the transition at T_0 got rapidly obscured by the resistivity drop at T_c upon applying field. The residual resistivity ratio (RRR) increases from ~1.3 in the old batch to ~2.8 in the new batch.

The low-temperature specific heat of $CeRh_2As_2$ at different fields is shown in Fig. 3 (see the SM for an extended data set [28]). Besides the pronounced peaks at T_c and T_0, there are no visible signatures of other phase transitions. Therefore, the existence of the AFM order inside the SC phase [13] would imply that $T_c = T_N$. Both T_c and T_0 anomalies shift to lower temperatures upon applying magnetic field, with the T_0 signature no longer apparent above 5 T. We used the equal-entropy construction for rigorously defining T_c and T_0 (detailed in the SM [28]).

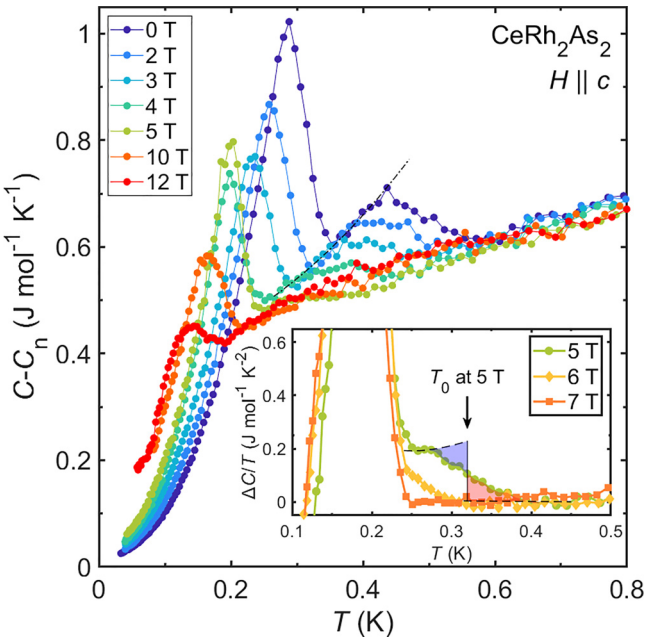

FIG. 3. Electronic specific heat $C - C_n$ of $CeRh_2As_2$ (new batch) against temperature T, measured at different c-axis magnetic fields. The dashed-dotted line marks the envelope curve of $C - C_n$ between the onset of superconductivity and the termination of the phase-I transition. Inset: Disappearance of the phase-I transition signature in specific heat. The extrapolated unordered state specific heat was subtracted to emphasize the anomalies. For 5 T, a plateau between 0.25 and 0.28 K indicates that the phase-I transition is complete before the superconductivity sets in, and the critical temperature T_0 can be determined via the shown equal-entropy construction.

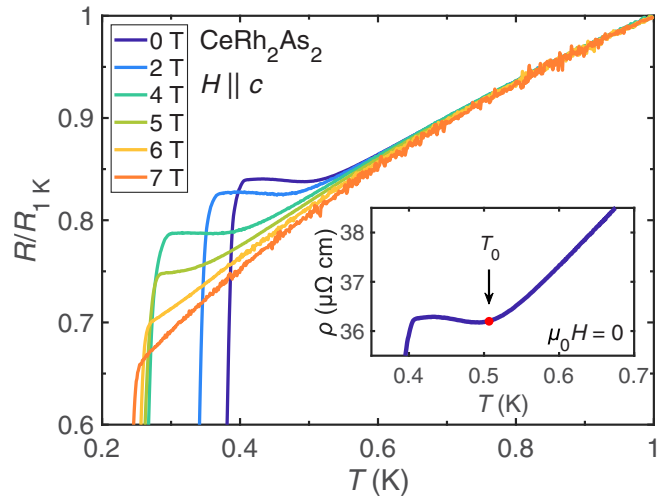

FIG. 4. Electrical resistance R against temperature T for $CeRh_2As_2$ samples of the new batch, normalized to the resistance at 1 K, for different c-axis magnetic fields. The inset displays zero-field resistivity $\rho(T)$ at the phase-I transition. The critical temperature T_0 was defined as the point of largest curvature (red dot).

The specific heat jump height at T_c exhibits a sharp increase as a function of field in a small interval around 4 T because of the kink in the SC phase boundary line at the multicritical point at H^* (as discussed in Ref. [1] and demonstrated in the SM [28]). It is also instructive to look at the evolution of specific heat for 5 T $\leqslant \mu_0 H \leqslant$ 7 T, shown in the inset of Fig. 3. In this field range, T_c is nearly constant. The phase-I transition is complete before the onset of superconductivity at 5 T, is interrupted at 6 T, and fully vanishes at 7 T. At the same time, the peak value of specific heat at T_c remains constant with respect to the unordered state ($T > T_0$). The disappearance of the T_0 signature between 5 and 6 T is accompanied by a slight increase of specific heat below T_c.

We also investigated the behavior of phase I and superconductivity in the field by measuring the electrical resistivity for current parallel to the basal plane of the $CeRh_2As_2$ lattice. The resultant data for selected values of H are shown in Fig. 4 (the extended data set is available in the SM [28]). The phase-I transition is identifiable as a pronounced upturn in $\rho(T)$ below ~0.6 K. In zero field, upon subsequent cooling, the upturn is followed by a downturn and the eventual SC transition. We defined T_0 as the point of maximum curvature of $\rho(T)$ (red dot in the Fig. 4 inset; see the SM [28] for details on determining T_0). The resultant boundary of phase I decently reproduces that obtained from specific heat measurements, as will be shown next.

We now discuss the T-H phase diagram of $CeRh_2As_2$ shown in Fig. 5. It summarizes the results of our specific heat and resistivity measurements conducted on samples from the new batch. The general shape of all phases—phase I, SC1, and SC2—is consistent with the previously published data [1,26]. While the transition temperatures are higher compared to the earlier generations of samples, the critical field $\mu_0 H^*$ between

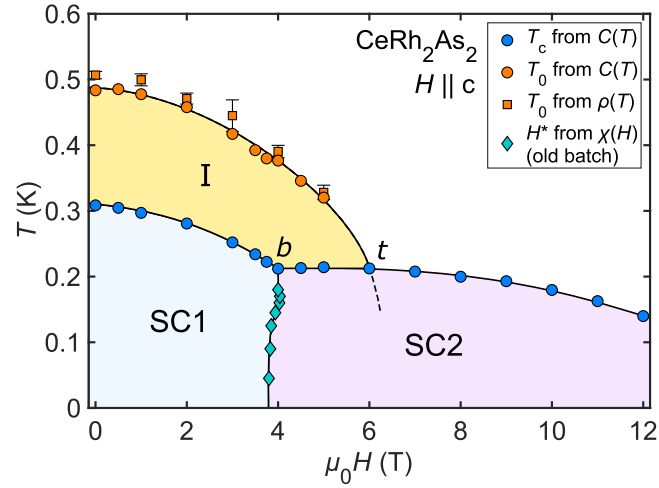

FIG. 5. Temperature–c-axis magnetic field (T-H) phase diagram of $CeRh_2As_2$ depicting the two superconducting (SC) states SC1 and SC2 and the ordered phase I. The SC and phase-I transition temperatures (T_c and T_0, respectively) come from measurements of specific heat $C(T)$ and electrical resistivity $\rho(T)$ conducted on samples from the new batch. The SC1-SC2 phase boundary, terminating in a bicritical point b, is plotted according to earlier ac magnetic susceptibility $\chi(H)$ data [1]. The solid black lines are guides for the eye. The dashed line marks a segment of a so far undetected hypothetical phase boundary expected from thermodynamic considerations, while t marks the corresponding tetracritical point.

SC1 and SC2 remains unchanged at 4 T. The zero-temperature limit of the SC upper critical field extrapolates to roughly 15 and 18 T for specific heat and resistivity, respectively. We can clearly identify T_0 at fields as high as 5 T, which was not possible in previous studies. The $T_0(H)$ line intercepts the SC2 phase boundary at approximately 6 T. Consequently, we can definitively conclude that the boundary of phase I does not meet the multicritical point at $\mu_0 H^* = 4$ T and is not responsible for the associated phase transition.

According to thermodynamic considerations [27], it is not possible to have a multicritical point at some field H_c, such that two second-order phase boundaries come out of it for $H < H_c$ and one phase boundary (first or second order) comes out for $H > H_c$ (holds true if the inequalities are swapped). Therefore, the point where the SC1 and SC2 phase boundaries meet is a bicritical one (labeled with the letter *b* in Fig. 5), and the SC1-SC2 transition must be of the first order. Applied to the crossing of the $T_c(H)$ and $T_0(H)$ lines at 6 T, this constraint requires that the boundary of phase I continues inside the SC2 state, resulting in a tetracritical point (indicated by the letter *t* in Fig. 5). That said, we do not observe any signature of the phase I within the SC2 phase (cf. the 7-T curve in the inset of Fig. 3). Given the steep slope of the $T_0(H)$ line near 6 T, it is quite possible that the transition evaded detection due to being too broad or the field sampling period of 1 T being too large.

We analyzed the experimental phase diagram using the Ginzburg-Landau (GL) theory of coupled order parameters [31], as done, e.g., for iron pnictide superconductors in Ref. [32]. The coupling term in the free energy between the SC2 and phase-I order parameters, Δ and $\mathbf{Q}$ respectively, is given by $\lambda\Delta^2\mathbf{Q}^2$, where λ indicates the strength of the coupling as well as its nature, $\lambda > 0$ for competing and $\lambda < 0$ for supporting coupling. We reproduced our experimental phase diagram by using the values of the transition temperatures, the slopes of the phase boundary lines, and the jumps of the specific heat coefficients at the transition temperatures, $\Delta C(T_0)/T_0$ and $\Delta C(T_c)/T_c$, which are directly related to the condensation energies and to the changes in the slopes of the $T_0(H)$ and $T_c(H)$ lines at *t*. A detailed analysis is provided in the SM [28]; here, we summarize the main findings: (i) The absence of a pronounced kink in the $T_c(H)$ line at *t* implies that the coupling is not strong. (ii) The supporting coupling is unlikely, since it flattens the $T_0(H)$ line below *t* [Fig. S9(d)], and we should have then observed a double feature in $C(T)/T$ at 7 T. (iii) In case of a weak competition, the slope change across *t* would be about two orders of magnitude larger for the $T_0(H)$ line than for the $T_c(H)$ line [Fig. S9(a)]. This is due to the fact that the changes of the slopes at *t* are related to $\Delta C(T_0)/T_0$ and $\Delta C(T_c)/T_c$ evaluated at *t*, and in our case $\Delta C(T_0)/T_0 \approx \frac{1}{10}\Delta C(T_c)/T_c$. For example, for λ equal to 20% of the value necessary to induce a first-order transition, the critical field of the phase I at $T = 0$ would go down by about 0.4 T compared to the case of no coupling, resulting in no phase-I-related feature observable in specific heat at 7 T. At the same time, T_c should slightly increase between the *b* and *t* points. Below the line joining *b* and *t*, the two states would then homogeneously coexist [32]. We indeed observe a slight change in the slope of T_c at *t* (see Fig. S10), consistent with the weak-coupling scenario, but extraction of quantitative information is hindered by the insufficient resolution of our data.

Whereas in iron pnictides both superconductivity and magnetism originate from the same FS sheet, the situation in $CeRh_2As_2$ is more complex due to the presence of two relevant sheets. The most reliable renormalized band structure calculations so far [10] predict a quasi-three-dimensional strongly corrugated cylinder (3D sheet) along the Γ-*Z* direction of the Brillouin zone (BZ) and quasi-two-dimensional corrugated cylinders (2D sheet) along axes parallel to the *A*-*M* direction. Within the parity change picture of the SC1-SC2 transition, the SC pairing is mainly driven by the electrons of the 2D sheet, located at the edges of the BZ, where the spin-orbit coupling dominates over the interlayer hopping [16]. A recent study [26] demonstrated that the upturn of $\rho(T)$ at T_0 is stronger when the current flows along the *c* axis as opposed to the *ab* plane. Within the QDW scenario, the associated FS nesting vector must therefore have a sizable out-of-plane component, and the states involved in the QDW instability are expected to belong to the 3D sheet of the FS. The attribution of the two orders to the different FS sheets disfavors a strong coupling between the QDW and superconductivity, and one would then expect the $T_0(H)$ line to continue into the SC2 phase practically undisturbed.

To conclude, using higher-quality crystals we refined the *T*-*H* phase diagram of $CeRh_2As_2$ for field parallel to the *c* axis, and showed that the phase-I boundary unambiguously does not meet the bicritical point between the two SC phases and is therefore not responsible for the SC1-SC2 transition. The $T_0(H)$ line intercepts the SC2 phase boundary at a tetracritical point near 6 T. Our analysis of the phase boundaries near the tetracritical point suggests a weak competing interaction between the SC and phase-I order parameters. These conclusions leave us with two viable explanations for the origin of the SC1-SC2 transition: the even-to-odd parity switching [1,15] or a change in magnetic ordering [24]. Our results prompt a further study of the 6 T tetracritical point, from which an additional phase boundary is expected to emerge.

We are indebted to D. Agterberg, D. Aoki, S. Kitagawa, G. Knebel, K. Ishida, A. P. Mackenzie, A. Rost, O. Stockert, Y. Yanase, and G. Zwicknagl for useful discussions. This work is also supported by the joint Agence National de la Recherche and DFG program Fermi-NESt through Grant No. GE602/4-1 (C.G. and E.H.). Additionally, E.H. acknowledges funding by the DFG through CRC1143 (Project No. 247310070) and the Würzburg-Dresden Cluster of Excellence on Complexity and Topology in Quantum Matter - ct.qmat (EXC 2147, project ID 390858490).

[1] S. Khim, J. F. Landaeta, J. Banda, N. Bannor, M. Brando, P. M. R. Brydon, D. Hafner, R. Küchler, R. Cardoso-Gil, U. Stockert *et al.*, Science **373**, 1012 (2021).

[2] R. A. Fisher, S. Kim, B. F. Woodfield, N. E. Phillips, L. Taillefer, K. Hasselbach, J. Flouquet, A. L. Giorgi, and J. L. Smith, Phys. Rev. Lett. **62**, 1411 (1989).

[3] G. Bruls, D. Weber, B. Wolf, P. Thalmeier, B. Lüthi, A. de Visser, and A. Menovsky, Phys. Rev. Lett. **65**, 2294 (1990).
[4] S. Adenwalla, S. W. Lin, Q. Z. Ran, Z. Zhao, J. B. Ketterson, J. A. Sauls, L. Taillefer, D. G. Hinks, M. Levy, and B. K. Sarma, Phys. Rev. Lett. **65**, 2298 (1990).
[5] D. Braithwaite, M. Vališka, G. Knebel, G. Lapertot, J. P. Brison, A. Pourret, M. E. Zhitomirsky, J. Flouquet, F. Honda, and D. Aoki, Commun. Phys. **2**, 147 (2019).
[6] D. Aoki, F. Honda, G. Knebel, D. Braithwaite, A. Nakamura, D. Li, Y. Homma, Y. Shimizu, Y. J. Sato, J.-P. Brison *et al.*, J. Phys. Soc. Jpn. **89**, 053705 (2020).
[7] K. Kinjo, H. Fujibayashi, S. Kitagawa, K. Ishida, Y. Tokunaga, H. Sakai, S. Kambe, A. Nakamura, Y. Shimizu, Y. Homma *et al.*, Phys. Rev. B **107**, L060502 (2023).
[8] H. Sakai, Y. Tokiwa, P. Opletal, M. Kimata, S. Awaji, T. Sasaki, D. Aoki, S. Kambe, Y. Tokunaga, and Y. Haga, Phys. Rev. Lett. **130**, 196002 (2023).
[9] A. W. W. Ludwig and I. Affleck, Phys. Rev. Lett. **67**, 3160 (1991).
[10] D. Hafner, P. Khanenko, E.-O. Eljaouhari, R. Küchler, J. Banda, N. Bannor, T. Lühmann, J. F. Landaeta, S. Mishra, I. Sheikin *et al.*, Phys. Rev. X **12**, 011023 (2022).
[11] J. Effantin, J. Rossat-Mignod, P. Burlet, H. Bartholin, S. Kunii, and T. Kasuya, J. Magn. Magn. Mater. **47-48**, 145 (1985).
[12] J. Kitagawa, N. Takeda, and M. Ishikawa, Phys. Rev. B **53**, 5101 (1996).
[13] M. Kibune, S. Kitagawa, K. Kinjo, S. Ogata, M. Manago, T. Taniguchi, K. Ishida, M. Brando, E. Hassinger, H. Rosner *et al.*, Phys. Rev. Lett. **128**, 057002 (2022).
[14] S. Ogata, S. Kitagawa, K. Kinjo, K. Ishida, M. Brando, E. Hassinger, C. Geibel, and S. Khim, Phys. Rev. Lett. **130**, 166001 (2023).
[15] J. F. Landaeta, P. Khanenko, D. C. Cavanagh, C. Geibel, S. Khim, S. Mishra, I. Sheikin, P. M. R. Brydon, D. F. Agterberg, M. Brando *et al.*, Phys. Rev. X **12**, 031001 (2022).
[16] D. C. Cavanagh, T. Shishidou, M. Weinert, P. M. R. Brydon, and D. F. Agterberg, Phys. Rev. B **105**, L020505 (2022).
[17] T. Yoshida, M. Sigrist, and Y. Yanase, Phys. Rev. B **86**, 134514 (2012).
[18] M. Sigrist, D. F. Agterberg, M. H. Fischer, J. Goryo, F. Loder, S.-H. Rhim, D. Maruyama, Y. Yanase, T. Yoshida, and S. J. Youn, J. Phys. Soc. Jpn. **83**, 061014 (2014).
[19] D. Möckli, Y. Yanase, and M. Sigrist, Phys. Rev. B **97**, 144508 (2018).
[20] E. G. Schertenleib, M. H. Fischer, and M. Sigrist, Phys. Rev. Res. **3**, 023179 (2021).
[21] A. Skurativska, M. Sigrist, and M. H. Fischer, Phys. Rev. Res. **3**, 033133 (2021).
[22] K. Nogaki, A. Daido, J. Ishizuka, and Y. Yanase, Phys. Rev. Res. **3**, L032071 (2021).
[23] K. Nogaki and Y. Yanase, Phys. Rev. B **106**, L100504 (2022).
[24] K. Machida, Phys. Rev. B **106**, 184509 (2022).
[25] O. P. Squire, S. A. Hodgson, J. Chen, V. Fedoseev, C. K. de Podesta, T. I. Weinberger, P. L. Alireza, and F. M. Grosche, arXiv:2211.00975 [Phys. Rev. Lett. (to be published)].
[26] S. Mishra, Y. Liu, E. D. Bauer, F. Ronning, and S. M. Thomas, Phys. Rev. B **106**, L140502 (2022).
[27] S. K. Yip, T. Li, and P. Kumar, Phys. Rev. B **43**, 2742 (1991).
[28] See Supplemental Material at http://link.aps.org/supplemental/10.1103/PhysRevB.107.L220504 for extended sets of resistivity and heat capacity data as well as additional details on the sample synthesis, data analysis, and application of the Ginzburg-Landau theory, which includes Refs. [33–36].
[29] S. Onishi, U. Stockert, S. Khim, J. Banda, M. Brando, and E. Hassinger, Front. Electron. Mater. **2**, 880579 (2022).
[30] M. D. Bachmann, G. M. Ferguson, F. Theuss, T. Meng, C. Putzke, T. Helm, K. R. Shirer, Y.-S. Li, K. A. Modic, M. Nicklas *et al.*, Science **366**, 221 (2019).
[31] Y. Imry, J. Phys. C **8**, 567 (1975).
[32] R. M. Fernandes and J. Schmalian, Phys. Rev. B **82**, 014521 (2010).
[33] F. Pobell, *Matter and Methods at Low Temperatures* (Springer, Berlin, 2007).
[34] A. Steppke, M. Brando, N. Oeschler, C. Krellner, C. Geibel, and F. Steglich, Phys. Status Solidi B **247**, 737 (2010).
[35] T. Hagino, Y. Seki, S. Takayanagi, N. Wada, and S. Nagata, Phys. Rev. B **49**, 6822 (1994).
[36] T. Grüner, D. Jang, Z. Huesges, R. Cardoso-Gil, G. H. Fecher, M. M. Koza, O. Stockert, A. Mackenzie, M. Brando, and C. Geibel, Nat. Phys. **13**, 967 (2017).